M. ILHAN, R. SAMUR, H. DEMIRER, F. MINDIVAN

ISSN 0543-5846
METABK 54(2) 407-410 (2015)
UDC – UDK 546.431.883:661.18:535.37=111

PHOTOLUMINESCENCE AND CONCENTRATION QUENCHING OF Pr^{3+} DOPED $BaTa_2O_6$ PHOSPHOR

Received – Primljeno: 2014-06-24
Accepted – Prihvaćeno: 2014-10-20
Preliminary Note – Prethodno priopćenje

The pure and Pr^{3+} doped TTB-$BaTa_2O_6$ phosphors were obtained by the solid state reaction method at 1 425 °C for 20 hours. X-Ray Diffraction (XRD) and Scanning Electron Microscope (SEM) analyses confirmed a single phase of $BaTa_2O_6$ up to 10 mol % Pr_2O_3. SEM analysis also shows that $BaTa_2O_6$ grain size decreased with the increasing Pr_2O_3 concentration. The chemical composition of Pr^{3+} doped $BaTa_2O_6$ structures was confirmed by Energy Dispersive Spectroscopy (EDS) analysis. $BaTa_2O_6$:Pr^{3+} phosphors exhibited on a strong red emission at 620,9 nm, a green emission at 548,3 nm and a red emission at 655,2 nm. Emission intensity increased with Pr^{3+} doping concentration up to 1,5 mol %, then decreased due to concentration quenching.

Key words: $BaTa_2O_6$; TTB, Pr^{3+}; phosphors; solid state reaction

INTRODUCTION

The trivalent rare earth ions doped materials have attracted considerable interest due to their photoemission across the whole visible spectral range [1,2]. The bright luminescence of these phosphors made possible a new generation of lighting and display devices with good thermal and chemical stability, and safety in the use [3]. Praseodymium (Pr^{3+}) can be excited using blue light through the transitions from ground state ($^3H_4$) to the ^3P_J (J = 0, 1, 2) and $^1D_2$ multiplets. In most oxides, Pr^{3+} ions emit blue-green or red light from the $^3P_0$ level: blue-green lines at ~500 nm ($^3P_0 \rightarrow {}^3H_4$) and 545 nm ($^3P_0 \rightarrow {}^3H_5$), red emission lines at ~618 nm ($^3P_0 \rightarrow {}^3H_6$) and 650 nm ($^3P_0 \rightarrow {}^3F_2$) [4,5].

$BaTa_2O_6$ is one of the compounds in BaO-Ta_2O_5 system which has been studied because of its dielectric and photocatalytic properties [6,7]. Synthesis of $BaTa_2O_6$ has been carried out by many methods: flux [8], solid state, precipitation [9], and mechanochemical synthesis [10,11]. $BaTa_2O_6$ has three crystal structures: orthorhombic, tetragonal, and hexagonal. Tetragonal structure has a TTB (tetragonal tungsten bronze) type structure [8]. The TTB crystal structure is related to that of the potassium tungstate ($K_{0.475}WO_3$) [12].

In this study, the luminescence properties of Pr_2O_3 doped $BaTa_2O_6$ were investigated. Also, microstructural characterization was performed using XRD and SEM techniques.

MATERIALS AND METHODS

Pure and $BaTa_2O_6$:xPr^{3+} ($0,5 \leq x \leq 10$ mol %) materials were synthesized by the solid state reaction method. $BaCO_3$ with a purity of 99 % (Sigma-Aldrich) and Ta_2O_5 with a purity of 99,9 % (Alfa Aesar) powders were used as starting materials to obtain $BaTa_2O_6$. Pr_2O_3 with a purity of 99,9 % (Alfa Aesar) was used as a dopant. $BaCO_3$ and Ta_2O_5 powders were mixed with respect to the $BaTa_2O_6$ stoichiometry. This mixture was doped by using (0,5, 1,5, 2,5, 5 and 10 mol %) Pr_2O_3. The doped mixture was homogenized in an agate mortar with the addition of acetone. Prepared powders were taken into alumina crucibles then sintered for 20 hours at 1 425 °C under air atmosphere in an electric furnace.

The average crystallite sizes and phase compositions of the sintered powders were determined by X-ray diffractometer (XRD, Rigaku Corp., D-MAX 2200) using Cu K_α radiation between 2θ = 15 – 60 ° at 2 °/min scan speed using the Ni filter. The average crystallite sizes of the powders were calculated using the Scherrer Formula (1) [13]:

$$D = \frac{k \cdot \lambda}{B \cdot \cos\theta} \quad (1)$$

Where D is mean crystallite size (nm); k is a constant (taken as 0,9); λ = 0,15406, the wavelength of CuK_α; B is the full width at half maximum (rad.); θ is the angle (°) between incident and diffracted beams. Morphology of the sintered powders was investigated by the Scanning Electron Microscopy (SEM, JEOL Ltd., JSM-5910LV) equipped with EDS (OXFORD Industries INCAx-Sight 7274; 133-eV resolution 5,9 keV) after Au-Pd coating. Photoluminescence measurements, excitation and emission spectra were recorded by Scinco floromaster-FS/2 model fluorometer with a Xe-arc lamp (150 W) as the excitation source. Photoluminescence (PL) analyses were performed at room temperature.

M. İlhan, Engineering Faculty, R. Samur, Faculty of Technical Education, H. Demirer, Technology Faculty, Marmara University, İstanbul, Turkey; F. Mindivan, S. E. University, Bilecik, Turkey

RESULTS AND DISCUSSION

Figure 1 shows the XRD patterns of pure and doped powders. XRD patterns of $BaTa_2O_6$ showed a TTB-$BaTa_2O_6$ single phase (JCPDS card No.17-0793) up to 10 mol % Pr_2O_3. A secondary phase was not observed. This shows that Pr^{3+} ions successfully incorporated into the TTB framework. XRD analysis indicated that powders crystallized in a tetragonal symmetry with space group *P4/mbm* having the TTB type structure. The cell parameters of tetragonal $BaTa_2O_6$ were reported as a = 12,52 Å, c = 3,956 Å, V = 620,10 Å^3 [8] and Z = 10 [14].

Table 1 **Average crystallite and grain size.**

Pr^{3+} conc. / mol %	Crystallite size / nm	Grain size / μm
Pure	42,47	0,8 - 4,4
0,5	38,51	0,7 - 4,2
1,5	35,20	0,6 - 4,0
2,5	32,60	0,5 - 3,7
5	30,12	0,5 - 3,4
10	27,30	0,4 - 3,2

The average powder crystallite size along doping concentration was calculated by using Scherrer's equation. The size of crystallites was given in Table 1. The crystallite size of the undoped powder was around 42 nm after 20 h of sintering. The crystallite size decreased with Pr^{3+} concentration and varied from 38 nm to 27 nm for doping levels of 0,5 and 10 % respectively.

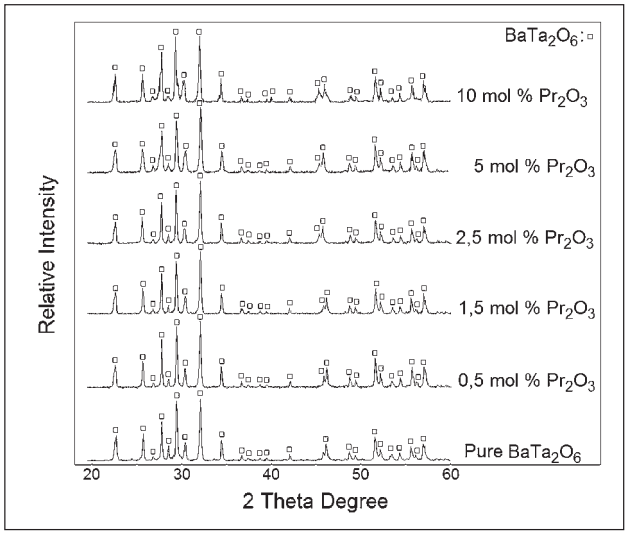

Figure 1 X-ray diffraction patterns of pure and Pr_2O_3 doped $BaTa_2O_6$ samples

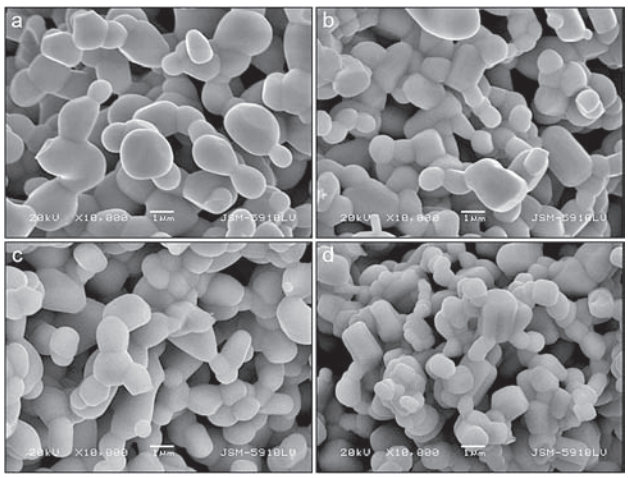

Figure 2 SEM micrographs of $BaTa_2O_6$ doped with Pr_2O_3 at (a) 0,5 %, (b) 2,5 %, (c) 5 % and (d) 10 mol %

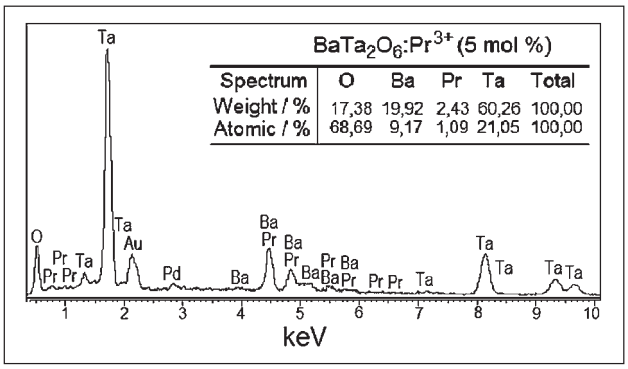

Figure 3 EDS analysis for Pr_2O_3 at 5 mol %

SEM-EDS observations confirmed the XRD findings. Figure 2 (a, b, c and d) shows the SEM micrographs of $BaTa_2O_6$ with different doping concentrations. The size of grains was shown in Table 1. The average grain size decreased with the in the Pr_2O_3 concentration. For all powders, grain sizes varied from submicron to a few microns. While the grain size of the pure powder ranges between 0,8 - 4,4 μm, it was 0,7 - 4,2 μm and 0,4 - 3,2 μm by Pr^{3+} doping up to 0,5 and 10 mol % respectively. All samples were found to have similar oval shaped grains. The EDS analysis revealed the differences in the chemical composition of grains. Figure 3 gives EDS spectrum of 5 mol % doped $BaTa_2O_6$ structure.

The excitation spectra of $BaTa_2O_6$:Pr^{3+} monitored at 620,9 nm, was shown in Figure 4. The spectra contained three excitation bands which were observed at $^3H_4 \rightarrow {}^3P_2$ (449,4 nm), $^3H_4 \rightarrow {}^3P_2$ (470,9 nm) and $^3H_4 \rightarrow {}^3P_0$ (486,5 nm) transitions. Among these bands, the peak at 470,9 nm was used to investigate the photoluminescence properties of different concentrations of Pr^{3+} ions in $BaTa_2O_6$:Pr^{3+} due to sharpness and intensity. Figure 5 shows the emission spectra of $BaTa_2O_6$:Pr^{3+} phosphors excited at 468,5 nm. Emission spectra $BaTa_2O_6$:Pr^{3+}

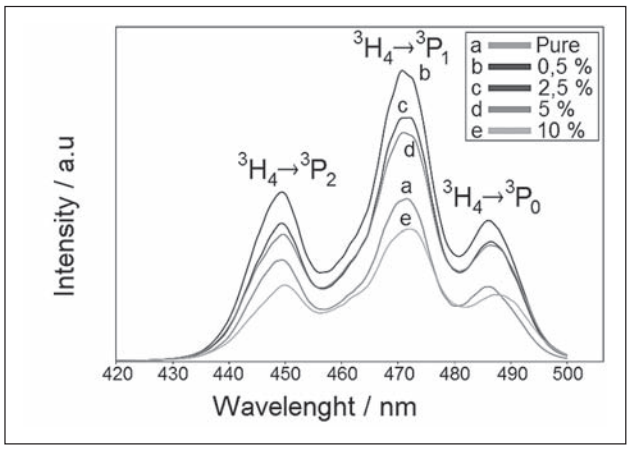

Figure 4 Excitation spectra of $BaTa_2O_6$:Pr^{3+} phophors at λ_{em} = 620,9 nm

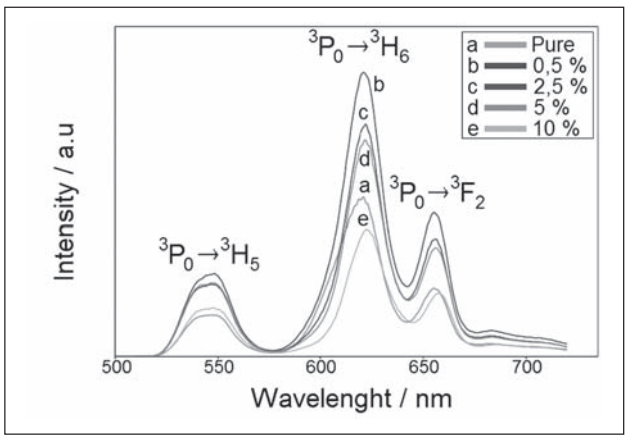

Figure 5 Emission spectra of $BaTa_2O_6:Pr^{3+}$ phosphors at λ_{ex}=468,5 nm

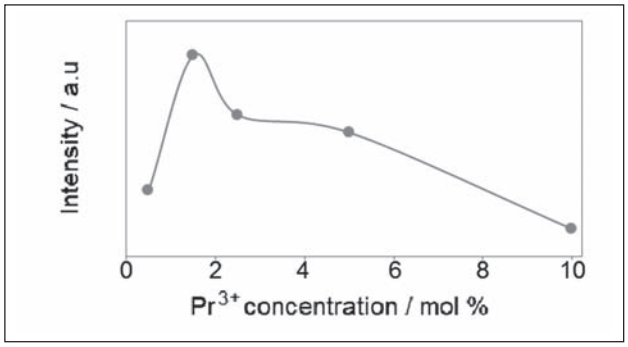

Figure 6 Emission intensity dependence of Pr^{3+} concentration for $BaTa_2O_6:Pr^{3+}$

phosphors exhibited three emissions: $^3P_0 \rightarrow {}^3H_5$, $^3P_0 \rightarrow {}^3H_6$ and $^3P_0 \rightarrow {}^3F_2$ for transitions at 548,3 nm, 620,9 nm, 655,2 nm respectively.

Figure 6 shows emission with the variation of Pr^{3+} doping concentration. Emission of Pr^{3+} ions increased with the increase of Pr^{3+} concentration up to 1,5 %, then decreased due to concentration quenching. When the concentration of Pr^{3+} ions increases, the distance between the Pr^{3+} ions decreases. This promotes non-radiative energy transfers between Pr^{3+} ions. XRD - SEM analyses may also support the idea of the decreased distance between Pr^{3+} ions through the decreased crystal and the grain size. Therefore, excitation energy transfer strongly depends on the distance between Pr^{3+} ions. Critical distance for energy transfer (R_c) in $BaTa_2O_6:Pr^{3+}$ can be estimated by Blasse formula (2) [15]:

$$R_c \approx 2\left(\frac{3V}{4\pi XcN}\right)^{1/3} \qquad (2)$$

where the structural parameters namely unit cell volume (V), the number of available sites for the dopant in the unit cell (N) and critical concentration of dopant (X_c). For the $BaTa_2O_6:Pr^{3+}$ phosphor, X_c = 0,015, V = 620,10 (Å)^3 and *(Z = 10)* N = 10. The R_c of Pr^{3+} in $BaTa_2O_6:Pr^{3+}$ was calculated as 19,92 Å. The non-radiative energy transfer of the luminescence of oxidic phosphors is based on the resonance transfer by electric multipole–multipole interaction or exchange interaction [16]. This situation was explained by the Blasse's theory [17]: When the critical distance is greater than 5 Å, only a multipole–multipole interaction is important where the exchange interaction becomes ineffective. When the distance is shorter than 5 Å, the exchange interaction becomes effective. Since the R_c value for $BaTa_2O_6:Pr^{3+}$ was calculated as 19,92 Å, the effective mechanism of concentration quenching of $BaTa_2O_6:Pr^{3+}$ phosphor was the multipolar interaction.

It is necessary to explain which type of interaction is related to the energy transfer and which enables the process of non-radiative energy transfers between Pr^{3+} ions due to the multipole–multipole interactions. According to Van Uitert [18], if the energy transfer occurs among the same sort of activators, the strength or type of the multipolar interaction can be determined from the change of the emission intensity and per concentration ion level that follows the equation (3):

$$I/x=K[1+\beta(x)^{\theta/3}]^{-1} \qquad (3)$$

In the equation, (x) is the phosphor concentration which is not less than the critical concentration. The (I/x) is the emission intensity *(I)* per phosphor *(x)*. The (K) and (β) are constants for the same excitation condition for a given phosphor crystal. The (θ) value indicates the electric multipolar character where $\theta = 3$ for the energy transfer among the nearest-neighbor ions (exchange interaction), while $\theta = 6$ dipole–dipole (d–d), $\theta = 8$ dipole–quadrupole (d–p) and $\theta = 10$ quadrupole–quadrupole (q–q) interactions. Assuming that $\beta(x)^{\theta/3} \gg 1$, equation (3) can be simplified as follows:

$$\log (I/x)=K'-\theta/3 \log x \quad (K'=\log K-\log \beta) \qquad (4)$$

The electric multipolar character (θ) can be obtained from the slope of equation (4), which is the slope ($-\theta/3$) of the plot log (I/x) and log (x). Critical concentration of Pr^{3+} has been determined to be 1,5 mol %. The dependence of the emission intensity of $BaTa_2O_6:Pr^{3+}$ phosphor excited at 470,9 nm as a function of the corresponding concentration of Pr^{3+} for concentration greater than the critical concentration ($x \geq 0{,}015$) is determined. The plot of log (I/x) as a function of log (x) for $BaTa_2O_6:Pr^{3+}$ phosphors were shown in Figure 7. It can be seen that the de-

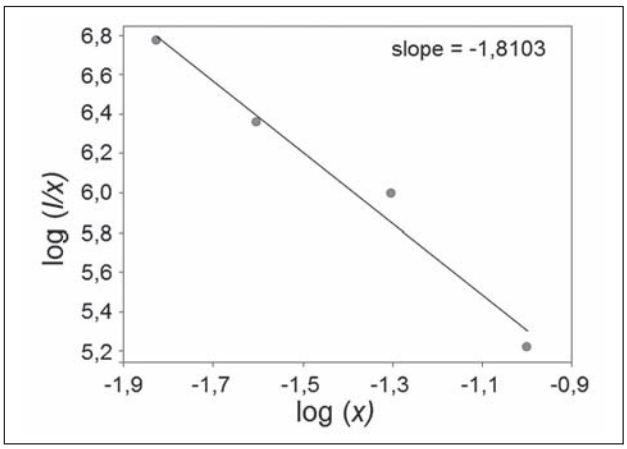

Figure 7 Relation between the $\log_{10}$(I/x) and $\log_{10}$(x) of Pr^{3+} for $BaTa_2O_6:xPr^{3+}$

pendence of log (*I/x*) on log (*x*) of Pr^{3+} is linear and its slope is around -1,8103. The value of θ can be calculated as 5,4309, which is nearly 6. This result indicates that the energy transfer mechanism for $BaTa_2O_6$:Pr^{3+} phosphor is a dipole–dipole (d–d) interaction.

CONCLUSION

A new light emitted Pr^{3+} doped $BaTa_2O_6$ was produced using the conventional solid state method. In the XRD results, TTB had a single phase that formed from 0,5 to 10 % Pr^{3+} doping concentration. In the SEM analysis, the $BaTa_2O_6$:Pr^{3+} grain size decreased depending on the Pr^{3+} concentration. $BaTa_2O_6$:Pr^{3+} exhibited a strong red emission at $^3P_0 \rightarrow {}^3H_6$ (620,9 nm) transition. While emission increased between 0,5 to 1,5 mol %, after that level emission decreased due to concentration quenching. The effective mechanism of quenching was found to be the dipole–dipole interaction since the critical distance is 19,92 Å. The results imply that the $BaTa_2O_6$:Pr^{3+} phosphor could be potentially used as red LEDs.

Acknowledgments

We would like to thank to the Marmara University Research Fund (Projects No: FEN-A-150513-0167 and FEN-D-090414-0105).

REFERENCES

[1] D. Balaji, A. Durairajan, D. Thangaraju, K. K. Rasu, S. M. Babu, Materials Science and Engineering B 178 (2013) 762-767.
[2] L. Qin, Y. Huang, T. Tsuboi, H. J. Seo, Mater. Res. Bull. 47 (2012) 4498-4502.
[3] D. Wang, Q. R. Yin, Y. X. Li, M. Q. Wang, J. Lumin. 97 (2002) 1-6.
[4] V. Gorbenko, Y. Zorenko, V. Savchyn, T. Zorenko, A. Pedan, V. Shkliarskyi, Radiation Measurements 45 (2010) 461-464.
[5] L. Wen,Y.L. Zhang, J. H. Yang, G.N. Wang, W. Chen, L. L. Hu, Acta. Phys. Sin-ch. Ed. (Chinese) 55 (2006) 1486.
[6] G. K. Layden, Mater. Res. Bull. 3 (1968) 349.
[7] H. Kato, A. Kudo, Chemical Physics Letters 295 (1998) 487-492.
[8] G. K. Layden, Mater. Res. Bull. 2 (1967) 533.
[9] S. C. Navale, V. Samuel, A. B. Gaikwad, V. A. Ravi, Ceram. Int. 33 (2007) 297–299.
[10] M. İlhan, A. Mergen, C. Yaman, Ceram. Int. 37 (2011) 1507-1514.
[11] M. İlhan, A. Mergen, C. Yaman, Ceram. Int 39 (2013) 5741-5750.
[12] Magneli, A., A.Ark. Kemi.1 (1949) 213-221.
[13] B. D. Cullity, S.R. Stock, Elements of X-ray Diffraction. third ed., Prentice Hall, USA, 2001.
[14] F. Brik, R. Enjalbert, C. Roucau, J. Galy, J. Solid State Chemistry 122 (1996) 7-14.
[15] G. Blasse, J. Solid State Chemistry 62 (1986) 207-211.
[16] G. Blasse, B.C. Grabmarier, Luminescent Materials. Springer - Verlag, Berlin, 1994, p. 99.
[17] G. Blasse, Philips Res. Rep. 24 (1969) 131.
[18] L. G. Van Uitert, J. Electrochem. Soc. 114 (1967) 1048-1053.

Note: The responsible translator for Engilsh language is Dr. Ö. F. Cantekin, School of Foreign Languages, Gazi University, Turkey.